JOURNAL OF MATERIALS SCIENCE 5 (1970) 752-761

Growth and Morphology of Large Single Crystals of Long Chain *n*-Paraffins and Ketones

D. BLOOR, G. D. DEAN*
Department of Physics, Queen Mary College, London E1 4NS

The physical properties of large single crystals of long chain *n*-paraffins and ketones would be of interest because of their structural similarity to polyethylene, but simple techniques for growing crystals from solution or the melt yield only small crystals. We have constructed a crystal growing apparatus using the predictions of Jackson's theory of growth morphology as a guide and, with high purity samples of $C_{23}H_{48}$ and $C_9H_{19}COC_9H_{19}$, have grown crystals with centimetre dimensions. The morphologies of the crystals are strikingly different. The hexagonal-orthorhombic phase transition in the paraffin produces a crystal with variable residual strain. The ketone has no phase transition and yields strain free crystals crossed by narrow strained regions.

1. Introduction

Single crystals of *n*-paraffins have previously been grown for X-ray and morphological studies [1-6]. These studies showed that certain of the *n*-paraffins have a similar crystal structure and morphology to polyethylene, a fact which has been helpful in the interpretation of the properties of this polymer [7-9]. The crystals, mostly grown from solution, were relatively small in size with dimensions of 1 to 2 mm or less, and our attempts to grow crystals by the Stockbarger and Czochralski techniques also produced crystals with maximum dimensions of 2 to 3 mm. For further work, on the far infra-red spectra of the *n*-paraffins and the related ketones, crystals were required with dimensions of 1 to 2 cm across and about 1 mm thick. In principle, growth from the melt can be used to grow large crystals of pure materials when the growth habit is known, so that the growth can be controlled [10]. Zone refining [11], chromatography [12] and other chemical techniques have resulted in the availability of purer organic materials and the Stockbarger technique has been used to grow large highly perfect crystals of some organic materials [13-15]. However, for many materials the growth morphology will render this method unsuitable. Organic materials, in fact, show a continuous range of habits from singular facets to interfaces determined only by the isotherms. This has resulted in their use as model systems to show the validity of Jackson's theory of growth morphology [16, 17]. In this work we have reversed this process and used the theory to guide the design of the crystal growing apparatus. The theoretical calculations are presented in section 2 and the crystal growing apparatus is described in section 3.

2. Calculation of the Growth Habits of *n*-Paraffins and Related Ketones

The morphology of macroscopic crystals growing from the melt is determined by the nature of the interface between melt and solid. Two possibilities exist, either a microscopically smooth interface or a microscopically rough interface. The former will produce a faceted crystal while the latter will result in growth forms determined purely by the thermal conditions during growth. The criteria for these two possibilities may be identified by the analysis of Jackson [16].

Growth is assumed to start from a smooth interface, i.e. a crystallographic plane, to which atoms are added in a random manner. The change in surface free energy, ΔF_S, produced by the addition of N_A atoms to a plane with N

*Present address: Division of Materials Applications, National Physical Laboratory, Teddington, Middlesex.

atoms is calculated. The expression obtained is:

$$\frac{\Delta F_s}{NkT_m} = \alpha \frac{N_A}{N^2}(N - N_A) - \ln\left[\frac{N}{N - N_A}\right] - \frac{N_A}{N}\ln\left[\frac{N - N_A}{N_A}\right] \quad (1)$$

where T_m is the melting temperature and α is a factor given by:

$$\alpha = \left[\frac{\Delta H}{kT_m}\right]\left[\frac{m'}{n}\right] \quad (2)$$

where ΔH is the latent heat of fusion and each atom has n nearest neighbours with m' of these in the growth plane. For $\alpha < 2.0$, N_A/N tends to 0.5, while for $\alpha > 2.0$, N_A/N tends to 0 or 1, i.e. for α less than two the surface is microscopically rough, while for α greater than two the surface remains a smooth lattice plane. The rate of growth of a rough interface is faster and occurs for a smaller super-cooling than that of a smooth interface [18] so that a small Jackson α for a particular lattice plane implies a fast growth (with an interface following the isotherms) while a large α implies a slow growth (but with a clearly defined facet). For compounds with simple structures the evaluation of the α-factors for different lattice planes is relatively easy. However, organic compounds, particularly those with large molecules, are more difficult because of the complexity of the intermolecular bonding.

The structure of a lattice of paraffin molecules depends upon the chain length of the molecule and whether the molecule contains an even or odd number of carbon atoms [2-4, 19-22]. For even paraffins up to C_{24} the stable (low temperature) structure is triclinic and up to C_{36} it is monoclinic. All odd paraffins, and even ones above C_{36}, are orthorhombic. The materials most fully studied here belong to this final group. The even paraffins undergo phase transitions at higher temperatures, and both even and odd paraffins pass into a hexagonal phase a few degrees below their melting temperature [23-25].

The evaluation of the α-factor for the paraffins is simplified by the fact that in the hexagonal phase the molecules are in free rotation about their long axis resulting in an averaging of the intermolecular forces [25]. Each CH_2 group can be treated as a unit with six equivalent neighbours in the basal (a-b) plane and six equivalent bonds. A chain with n units has $6n$ bonds along the length of the chain and one bond at each end linking it with the molecules in adjacent basal planes. Hence for growth on the basal plane:

$$\alpha_{(0001)} = \frac{\Delta H}{kT_m}\frac{6n}{6n + 2} \quad (3)$$

and for growth on {1100} facets:

$$\alpha_{\{1100\}} = \frac{\Delta H}{kT_m}\frac{2n + 2}{6n + 2} \quad (4)$$

Thus, $\alpha_{\{1100\}} < \alpha_{(0001)}$ and growth on the facets will be favoured to growth on the basal plane. Numerical values for $\alpha_{(0001)}$ and $\alpha_{\{1100\}}$ for three odd paraffins are listed in table I. These were calculated using the data of Shearer *et al* [26].

TABLE I

	$C_{19}H_{40}$	$C_{23}H_{48}$	$C_{27}H_{56}$
$\alpha_{(0001)}$	16.8	19.0	20.6
$\alpha_{\{110\}_0}$	5.9	6.6	7.1

These general expectations account for the morphology of small paraffin crystals produced by simple solution and melt methods. These are plates with the c-axis normal to the largest faces. The fact that large crystals could not be produced by these techniques is due to the likelihood of spurious nucleation of misorientated material on the slowly growing c-axis facets. For our pulled boules the usual necking and expansion did not produce a single crystal but a sheaf of randomly orientated crystals. This we now attribute to the slow growth along the c-axis, which cannot follow the expansion of the boule, and the large supercooling on this facet, which results in further nucleation. Such nucleation has been observed in other organic materials with large α-factors [17] and in extreme cases ($\alpha \simeq 50$) spontaneous nucleation of spherulitic growth occurs ahead of the melt solid interface. The α-factors deduced here indicate that random nucleation is certain on the (0001) face and possible on the {1100} faces. The pulled material shows random nucleation on (0001) faces only, indicating that the calculated values are a little too large. However, the conclusion, that the growth of large paraffin crystals will be possible only if growth along the c-axis is minimised, will still be valid.

Estimation of the α-factors for the ketones is less certain as the structures are not known. However, the behaviour of solid solutions of ketones and paraffins suggests that the ketones crystallise in the low temperature phase of the equivalent paraffin [27]. The presence of the

oxygen dipole on the paraffin backbone appears to prevent the free rotation of the molecule. Near the melting point the molecules are likely to have a large librational amplitude and this, together with the fact that the differences in the hexagonal and orthorhombic structures are small, suggests that the α-factors will be similar to those of the paraffins. Hence, as for the paraffins, minimisation of growth rate in the c-axis direction is essential for the elimination of spurious nucleation and the growth of large crystals.

3. Crystal Growth

In order to grow crystals with centimetre dimensions it is necessary, by the arguments of section 2, to suppress growth along the c-axis and, because of the large α-factors, the growth rate in the basal (a-b) must be kept small. The apparatus designed to fit this specification is shown in fig. 1. The melt is contained in a specially shaped perspex cell (fig. 2) constructed in two halves to allow extraction of the final solid charge. Growth takes place by reducing the temperature of the lower end of the cell. The very finely tapered base of the cell restricts the

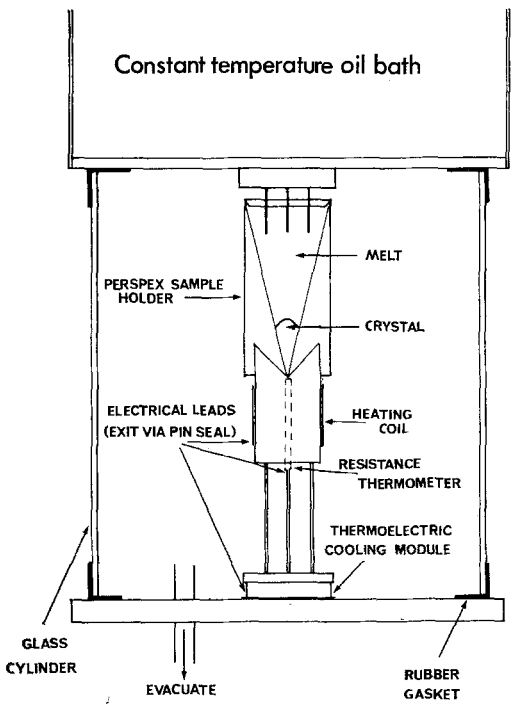

Figure 1 Cross section of the crystal growing apparatus. The heat shield connected to the oil bath has been omitted for clarity.

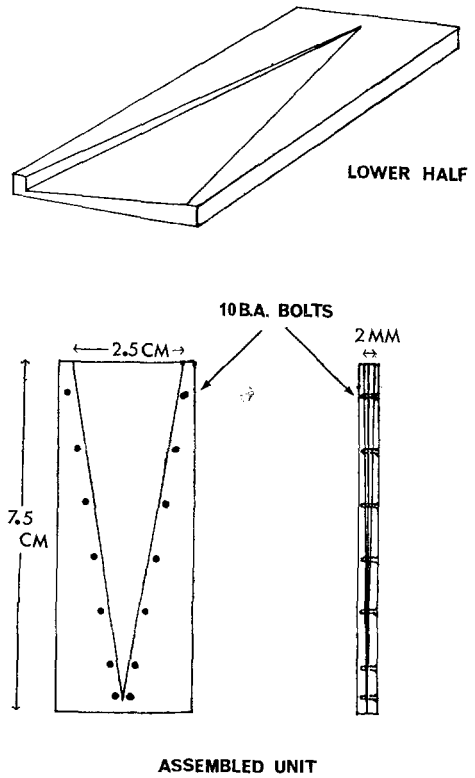

Figure 2 Structure and assembly of the perspex growth cell.

number of initial nuclei. Those nuclei which are orientated with their c-axis perpendicular to the large faces of the cell are favoured. In practice a single nucleation could be obtained by using a slow growth rate. The final crystals were all found to have the orientation described above.

The lower heater is supplied from a Eurotherm DHS temperature controller so that the temperature of the brass block, into which the cell is clamped, is kept constant to about one hundredth of a degree centigrade. The top heater is an oil bath controlled by a point contact thermometer. Thermal contact with the melt is provided by three pins dipping into the melt. The coupling is sufficient to maintain a melt in the cell but is poor enough to damp out the relatively large fluctuations in bath temperature. A heat shield of copper shim, soldered to this bath, surrounds the melt. This is designed to allow the melt to be observed during growth, to provide a linear temperature gradient along the cell and a lateral gradient giving a growth interface convex to the melt, thus preventing spurious nucleation affecting the growth. The temperature of the lower heater can be decreased by a Eurotherm pro-

gramming unit which allows the growth rate along the cell to be varied between 0.1 and 3 mm per hour. These correspond to growth rates along the *c*-axis of 3 μm and 0.1 mm per hour. The glass vessel can be evacuated to reduce the effect of external temperature fluctuations.

The cell is filled while just above the melting point of the charge material. This ensures that the charge is free from trapped gas bubbles. After inserting the cell into the growth apparatus the lower heater is set just above the melting point of the charge and the temperature of the oil bath raised until the whole charge is molten. The temperature of the lower heater is then reduced by the programming unit. Initial attempts failed due to the appearance of gas bubbles at the melt-solid interface. It was found that evacuation of the apparatus, while the charge was molten prior to initiation of growth, rapidly removed dissolved atmospheric gases from the charge. The melt continued to bubble, after the evolution of dissolved gas, under a vacuum of about 10^{-1} torr. Deposition of material on the glass vessel showed that the charge was evaporating. This was unexpected as previous work indicates a vapour pressure of 10^{-4} torr, or less near the melting points of the *n*-paraffins [28]. High vapour pressures were observed in this way for samples of varying purity. The low values previously reported may result from the inapplicability of the Knudsen method to vapours containing large anisotropic molecules and this matter would merit further study. To reduce this evaporation, helium gas was introduced at a pressure of about half an atmosphere. If any helium is absorbed by the melt it should be able to diffuse rapidly enough to prevent bubble formation at the melt-solid interface and in practice no bubbles were observed at the interface under these conditions. We found it possible to produce large crystals only from very pure starting materials. This suggests that the common impurities have large segregation coefficients so that even at very slow growth rates considerable constitutional supercooling occurs in the stagnant melt.

We were fortunate in being able to obtain very pure samples of *n*-tricosane ($C_{23}H_{48}$) from Dr M. J. Richardson [29], which had been purified by distillation until no impurities were detectable by gas-liquid chromatography. The lower heater is set at the melting point of the paraffin (49° C) and the oil bath heated to 65° C when the charge is molten. To initiate growth the temperature of the lower heater is decreased at about 0.4° C per hour. The solid that first forms in the cell is transparent, but on cooling to below 40.5° C the material becomes less clear, the phase transition from the hexagonal to the orthorhombic structure occurring at a clearly defined boundary. By using growth rates of less than 1 mm per hour it is possible to prevent the phase change from shattering the crystal. A sample of the ketone *n*-10-nonadecanone ($C_9H_{19}COC_9H_{19}$) of similar purity was obtained from Dr C. Burton [30]. The higher melting point of the ketone (59° C) necessitates initial heater and bath temperatures of 59 and 78° C respectively. The same cooling rate is used and a clear crystal, with no visible phase change on cooling to room temperature, is obtained. The perfection of these crystals is discussed in the next section.

4. Morphology of Melt Grown Crystals

The crystals were examined under the polarising microscope using both orthoscopic and conoscopic illumination. Measurements were made on free crystals since they were not affected by careful removal from the growth cell.

The hexagonal to orthorhombic phase transition has a marked effect on the perfection of the crystals of *n*-tricosane since the solid adheres to the cell and the highly anisotropic thermal expansion ($\alpha_a = 5 \times 10^{-4}$ deg.$^{-1}$, $\alpha_b = 1.6 \times 10^{-4}$ deg.$^{-1}$ [31]) produces a highly stressed material. Twinning can occur to reduce strains and in the initial thin section of the charge twins can be seen. As the thickness of the charge increases, the twin regions become larger and the whole of the upper section of the charge may be a single domain. Fig. 3 shows such a charge after removal of the initial twinned region. The thinnest section, on the right of fig. 3, is slightly strained and gives the optical figure shown in fig. 4. This shows that the *c*-axis is parallel to the direction of illumination, i.e. perpendicular to the largest faces of the growth cell. The optical figure has a constant orientation over the remainder of the charge, but as the thickness of the charge increases its quality decreases indicating an increasing amount of residual strain.

In order to obtain the best possible sample for the spectroscopic observations the least strained sections of crystal were cut from three boules and carefully aligned to ensure a single orientation. Far infra-red spectra were recorded using radiation polarised with the electric vector parallel to

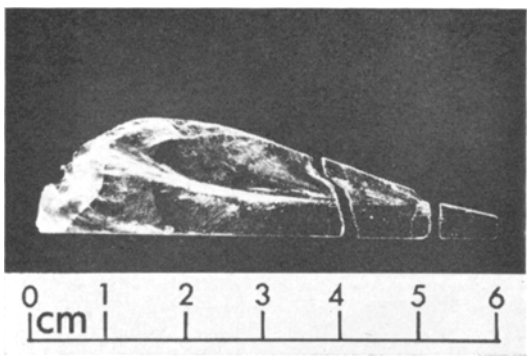

Figure 3 Single crystal of *n*-tricosane. The least strained section at the right gives the optical figure of fig. 4 and formed part of the sample used to obtain the far infra-red spectra. Apparent opacity is due to surface damage produced during removal from the growth cell. Increasing strain is shown by the crack propagated through the upper section of the crystal.

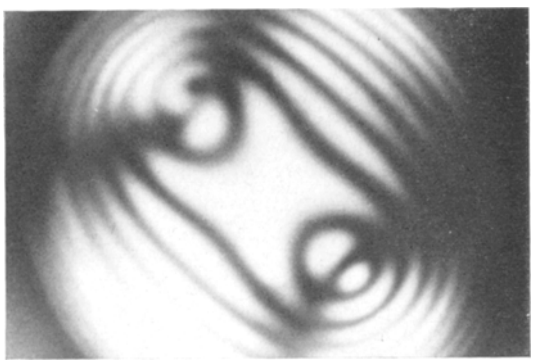

Figure 4 Optical figure of the least strained section of the crystal shown in fig. 3.

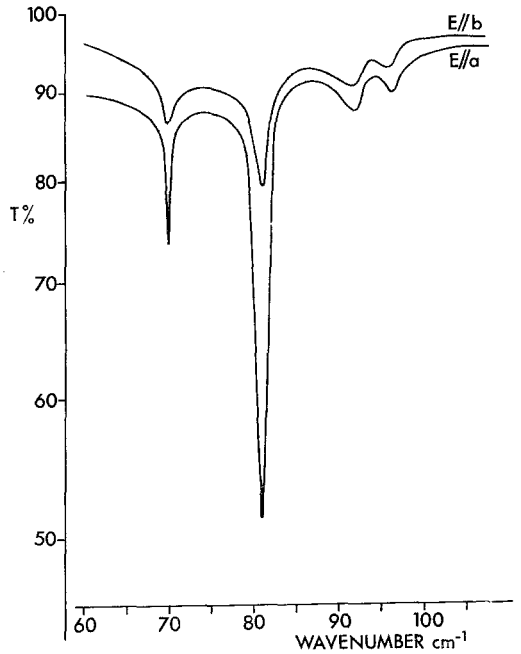

Figure 5 Far infra-red spectra of the composite sample of *n*-tricosane.

either the *a*- or *b*-axis. The results are shown in fig. 5. The assignment of the absorption bands can be made unambiguously and will be discussed elsewhere [32].

The absence of a phase transition for the *n*-10-nonadecanone gives a solid charge which is much less strained than the crystals of *n*-tricosane. The bulk of the charge is unstrained but is crossed by narrow highly strained regions. The

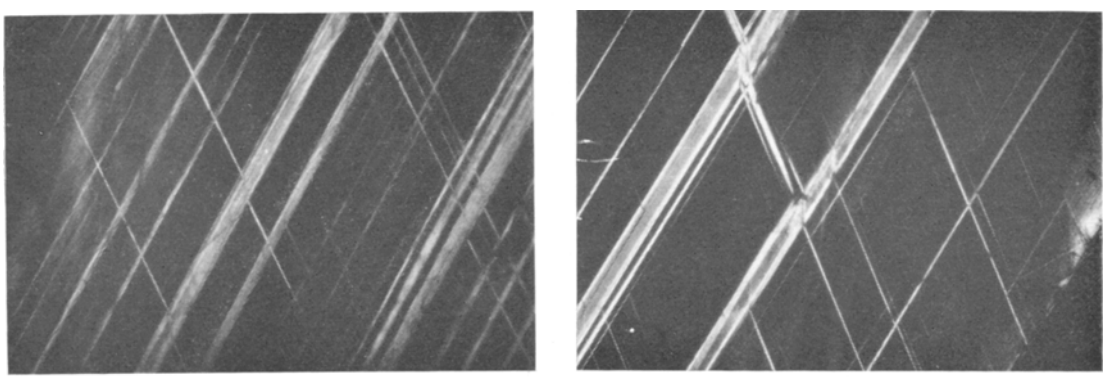

Figure 6 Photomicrographs of an *n*-10-nonadecanone crystal viewed under orthoscopic illumination. The microscope stage was translated linearly through about 3 cm between (a) and (b). The major features have (3 1 0) and (3 $\bar{1}$ 0) orientations, a few with (1 1 0) orientation are visible. The area shown is approximately 1.0 × 1.5 mm.

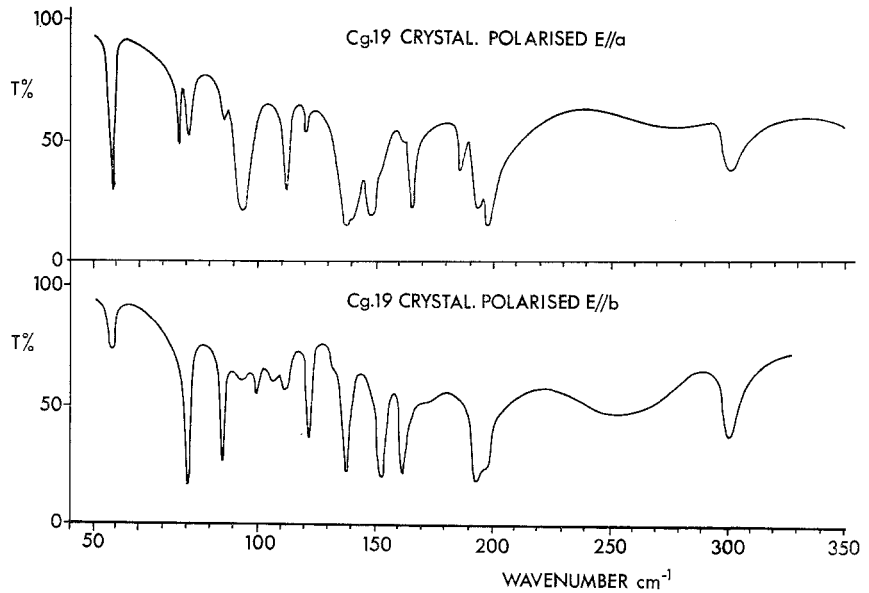

Figure 7 Far infra-red spectra of *n*-10-nonadecanone single crystal.

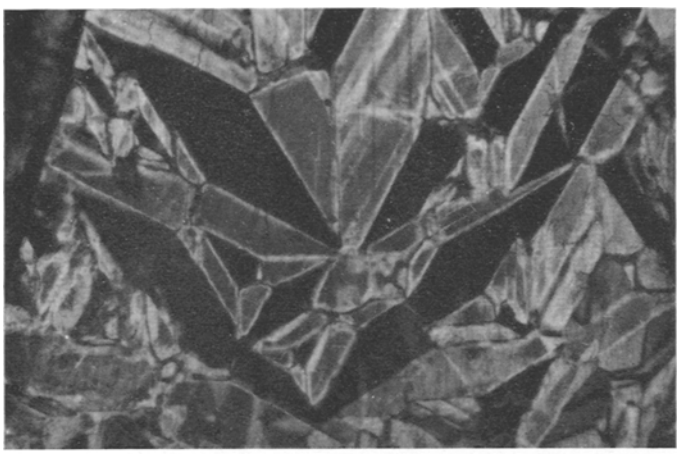

(a)

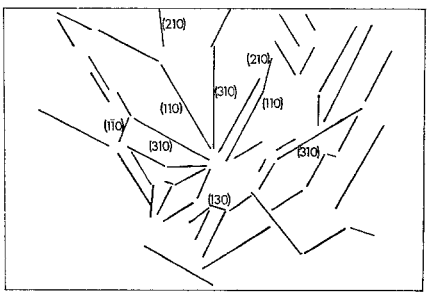

(c)

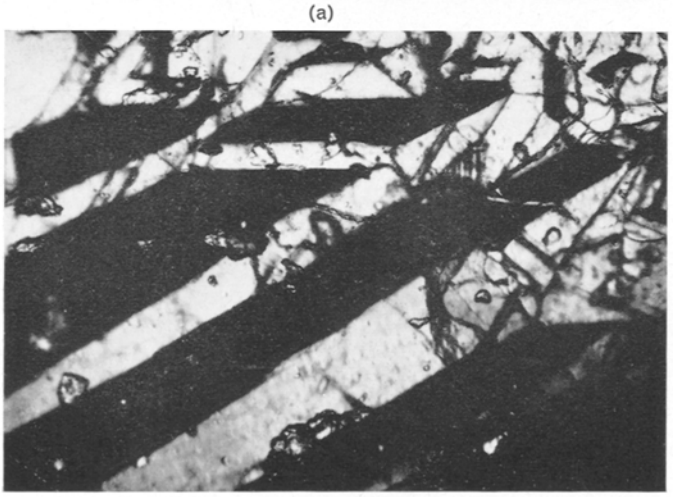

(b)

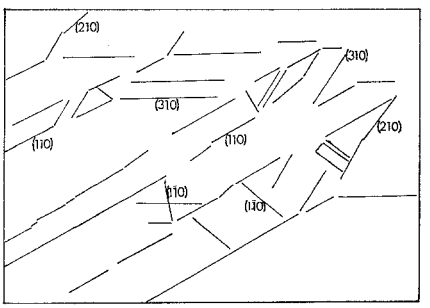

(d)

Figure 8 (a)-(b) Photomicrographs of the initial twinned section of *n*-tricosane boules viewed under orthoscopic illumination. Magnification is identical with that of fig. 6. (c)-(d) Orientations of twin boundaries in (a) and (b).

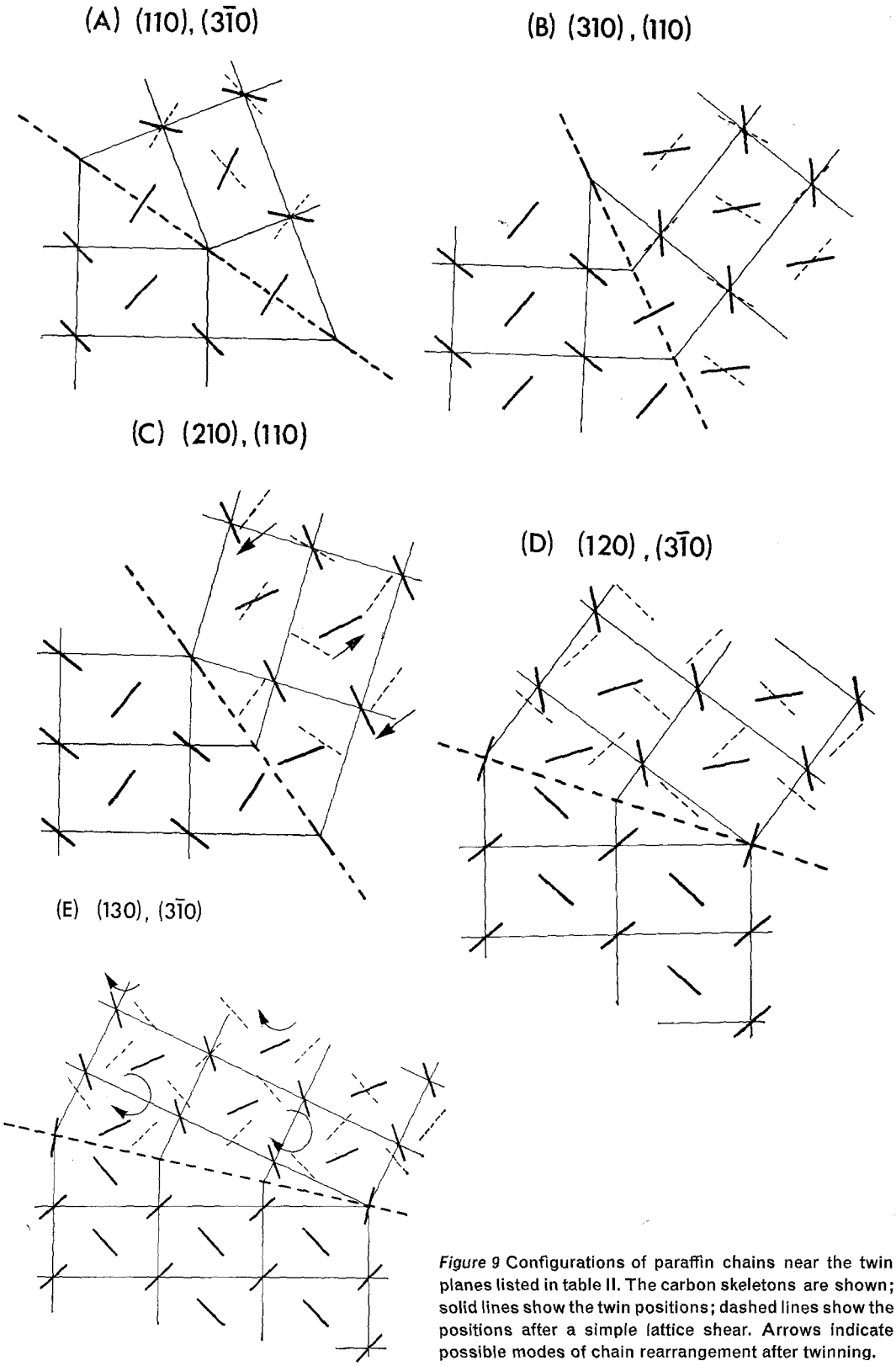

Figure 9 Configurations of paraffin chains near the twin planes listed in table II. The carbon skeletons are shown; solid lines show the twin positions; dashed lines show the positions after a simple lattice shear. Arrows indicate possible modes of chain rearrangement after twinning.

crystallinity of the charge is shown by a constant orientation of the optical figure of the strain free regions and of the features crossing the crystal (fig. 6). The stress produced on cooling by the anisotropic contraction of the charge relative to the cell, to which it adheres, has presumably been reduced by either deformation twinning or slip. Discs 2 cm in diameter can easily be cut from the crystal and far infra-red spectra were obtained, with radiation polarised along the *a*- and *b*-axes. These are shown in fig. 7. The spectrum is more complex than that of the paraffin because of the dipole moment associated with the C–O bond, these results will be discussed elsewhere [32]. The appearance of fully polarised lines in the spectra serve to confirm the high crystallinity of the sample.

Melt grown crystals of both materials are soft and waxy unlike solution grown crystals, which are relatively brittle. The starting materials used are of high purity (better than 99.9%) and the final crystals are free from absorbed solvent. The differences in mechanical properties are possibly a result of the differences in purity.

The twin features appearing in both materials were studied in detail. Structures similar to those of fig. 8 have been observed in impure paraffins by Kolvoort [33] and Keller [6], but have not been fully described. Measurements of the twin orientations show that the most common planes are (1 1 0) and (3 1 0), as reported by Kolvoort in $C_{24}H_{50}$. In addition (1 3 0) and (2 1 0) planes are observed to occur (fig. 8), but with a much lower frequency. These observations are in accord with the modes of deformation twinning reported by Frank *et al* [34] to occur in rolled polyethylene, and (1 1 0), (1 $\bar{1}$ 0), (3 1 0) and (3 $\bar{1}$ 0) orthorhombic planes are most likely on the basis of Mallard's law [35]. The problem of choice of twin plane has recently been generalised by Bilby and Crocker [36]. They show how to identify twin planes with low shear but the importance of lattice rearrangement for non-crystallographic shear is also emphasised. The twin modes listed in table II have shear less than 0.5.

Though the (2 1 0) mode has least shear it is less often observed than (1 1 0) and (3 1 0) modes, and, while the (1 2 0) mode has a shear close to that of the common modes it has not been observed. The chain arrangements for the modes listed in table II are shown in fig. 9. For (1 1 0) and (3 1 0) composition planes (or their conjugates) only small rotations of the paraffin chains are necessary, while for all other twin planes translation as well as rotation of the chains is required. However, in the case of (2 1 0) and (1 3 0) planes (and their conjugates) there is a relatively simple pattern of rearrangement, as seen in the figure. This is a likely explanation for their occurrence in preference to (1 2 0) planes, where a much less simple rearrangement is involved.

TABLE II

Composition plane (K_1)	Conjugate plane (K_2)	Shear direction (η_1)	Conjugate axis (η_2)	Shear (g)
(1 1 0)	(3 $\bar{1}$ 0)	[1 0 $\bar{1}$]	[1 3 0]	0.25
(3 1 0)	(1 $\bar{1}$ 0)	[1 $\bar{3}$ 0]	[1 1 0]	0.25
(2 1 0)	(1 $\bar{1}$ 0)	[1 $\bar{2}$ 0]	[1 1 0]	0.12
(1 2 0)	(3 $\bar{1}$ 0)	[$\bar{2}$ 1 0]	[1 3 0]	0.26
(1 3 0)	(3 $\bar{1}$ 0)	[$\bar{3}$ 1 0]	[1 3 0]	0.50

An X-ray examination of a *n*-10-nonadecanone single crystal showed that it has an orthorhombic structure identical to that of the *n*-paraffin of the same chain length [37]. The interpretations of the optical figure and features of the crystal are the same as those for the paraffin. The strained regions shown in fig. 6 are bounded by (3 1 0) and (1 1 0) planes (and their conjugates). This suggests that the features are deformation twins since these are the primary twin planes of the paraffin. A further point in favour of deformation twin formation, rather than slip, is that the most likely mode for slip should be that involving the shortest lattice vector as the Burgers vector, i.e. [0 1 0] (1 0 0) slip. This mode is not observed in slowly cooled crystals. The stress resulting from anisotropic contraction relative to the cell, assuming values for the expansion coefficients close to those of paraffins, is tension close to [1 0 0] (local adhesion will cause this to vary about a mean direction 10° off [1 0 0]), thus favouring the (3 1 0) and (1 1 0) twin modes. The macroscopic features could be composed of microscopic slip along the *a*- and *b*-axes, but the striking similarity of these features to deformation twins in certain metal systems argues against this. One sample was rapidly cooled to room temperature. There was considerable residual strain in this sample, comparable with that in the paraffin crystals, and numerous twin features. As well as features with (1 1 0) and (3 1 0) orientations, several with the other orientations observed in the paraffin ((1 3 0) and (2 1 0)), and others on (1 0 0) and (0 1 0) planes were apparent, see fig. 10. Twinning on the latter planes is

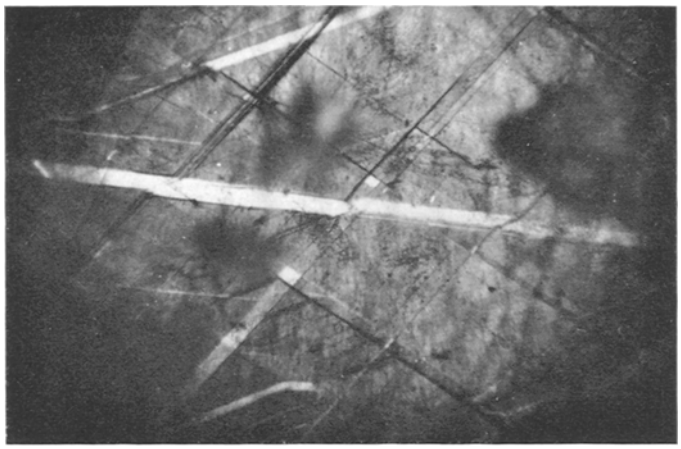

(a)

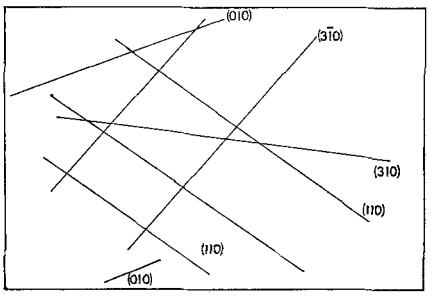

(d)

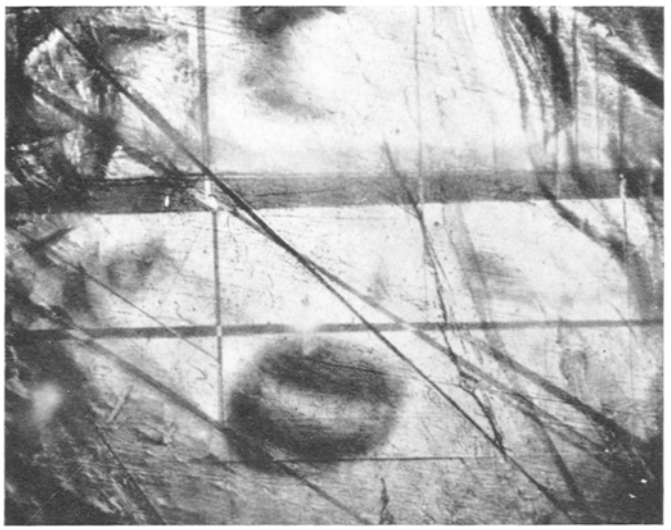

(b)

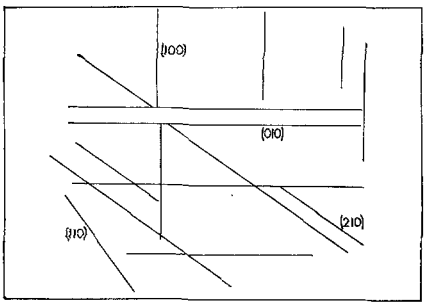

(e)

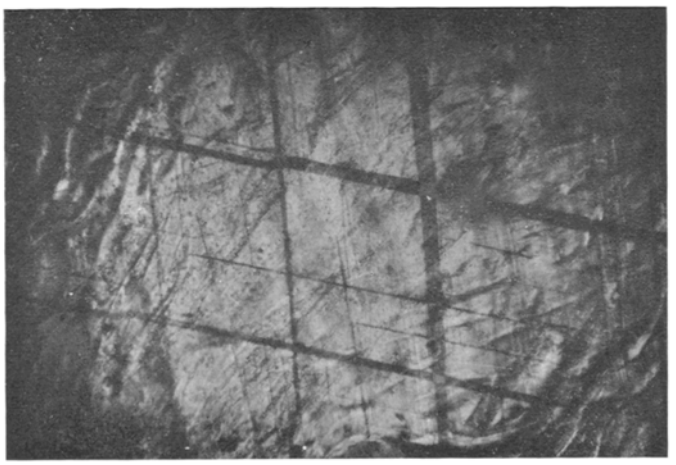

(c)

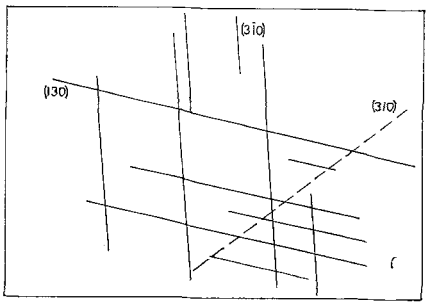

(f)

Figure 10 (a)-(c) Photomicrographs of rapidly cooled crystal of *n*-10-nonedecanone viewed under orthoscopic illumination. Magnification is identical with that of fig. 6. (d)-(f) Orientations of the bounding surfaces of the features in (a)-(c). The dashed line in (f) shows a feature visible in the original colour photograph. Features not shown in (d)-(f) are surface irregularities.

possible, by rotation of the molecules, but this will not relieve stress unless it is accompanied by some slip. These observations are in agreement with those made on the paraffin and serve to illustrate the importance of lattice rearrangement in determining the twin modes in these materials.

Acknowledgements

One of us (G.D.D.) thanks the Science Research Council for a Postgraduate Studentship. We thank Dr M. J. Richardson and Dr C. Burton for the supply of pure materials and Dr P. T. Clarke of the National Physical Laboratory for making the X-ray measurements of the ketone crystals.

References

1. A. MULLER, *Proc. Roy. Soc.* **114A** (1927) 542.
2. J. M. DAWSON and V. VAND, *ibid* **206A** (1951) 555.
3. M. H. M. SHEARER and V. VAND, *Acta Cryst.* **9** (1956) 379.
4. P. W. TEARE, *Acta Cryst.* **12** (1959) 294.
5. A. KELLER, *Makromal. Chem.* **34** (1959) 1.
6. *Idem, Phil. Mag.* **6** (1961) 329.
7. D. C. BASSET and A. KELLER, *ibid* **6** (1961) 345.
8. A. KELLER, *Reports on Progress in Phys.* **31** (1968) 623.
9. G. D. DEAN and D. H. MARTIN, *Chem. Phys. Letters* **1** (1967) 415.
10. W. A. TILLER, "Art and Science of Crystal Growth", edited by J. J. Gilman (J. Wiley & Sons, New York, 1963), p. 276.
11. W. G. PFANN, C. E. MILLER, and J. D. HUNT, *Rev. Sci. Instr.* **37** (1966) 649.
12. G. W. A. RIJNDERS, *Adv. Chromatog.* **3** (1966) 215.
13. J. N. SHERWOOD, "Crystal Growth", edited by H. S. Peiser (Pergamon Press, Oxford, 1967) p. 839.
14. N. T. CORKE, J. N. SHERWOOD, and R. C. JARNIGAN, *J. Cryst. Growth* **3, 4** (1968) 766.
15. I. I. STANIOU, *Stud. Cercetari Fiz.* **18** (1966) 201.
16. K. A. JACKSON, Liquid Metals and Solidification (*Amer. Soc. Met.*, Cleveland, 1958) p. 174.
17. *Idem*, "Crystal Growth", edited by H. S. Peiser (Pergamon Press, Oxford, 1967) p. 17.
18. J. C. BRICE, "The Growth of Crystals from the Melt" (North Holland, Amsterdam, 1965) p. 57.
19. I. M. DAWSON, *Proc. Roy. Soc.* **214A** (1952) 72.
20. *Idem, ibid* **218A** (1953) 255.
21. A. E. SMITH, *J. Chem. Phys.* **21** (1953) 2229.
22. S. M. OHLBERG, *J. Phys. Chem.* **63** (1958) 248.
23. V. DANIEL, *Adv. Phys.* **2** (1953) 450.
24. A. MULLER, *Proc. Roy. Soc.* **138A** (1932) 514.
25. D. W. MCCLURE, *J. Chem. Phys.* **49** (1968) 1830.
26. A. A. SHEARER, C. J. BUSS, A. E. SMITH, and L. B. SKINNER, *J. Amer. Chem. Soc.* **77** (1955) 2017.
27. R. J. MEAKINS, *Trans. Faraday Soc.* **55** (1959) 1694.
28. D. N. MORECROFT, *J. Chem. Eng. Data* **9** (1964) 488.
29. M. J. RICHARDSON, National Physical Laboratory, Teddington, Middlesex.
30. C. BURTON, National Standards Laboratory, Chippendale, N.S.W., Australia.
31. YU. V. MNYUKH, *Zhur. fiz. Khim.* **33** (1959) 1638 (Translation *Russ. J. Phys. Chem.* **33** (1959) 88).
32. G. D. DEAN and D. H. MARTIN, to be published.
33. E. C. H. KOLVOORT, *J. Inst. Petrol. Tech.* **24** (1938) 338.
34. F. C. FRANK, A. KELLER, and A. O'CONNOR, *Phil. Mag.* **3** (1958) 64.
35. F. C. FRANK, *Acta Metallurgica* **1** (1953) 71.
36. B. A. BILBY and A. G. CROCKER, *Proc. Roy. Soc.* **288A** (1965) 240.
37. P. T. CLARKE, private communication.

Received 22 February and accepted 10 July 1970.